



Fuzzy optimization model for enhanced weathering networks using industrial waste

Kathleen B. Aviso¹ · Jui-Yuan Lee² · Aristotle T. Ubando³ · Raymond R. Tan¹

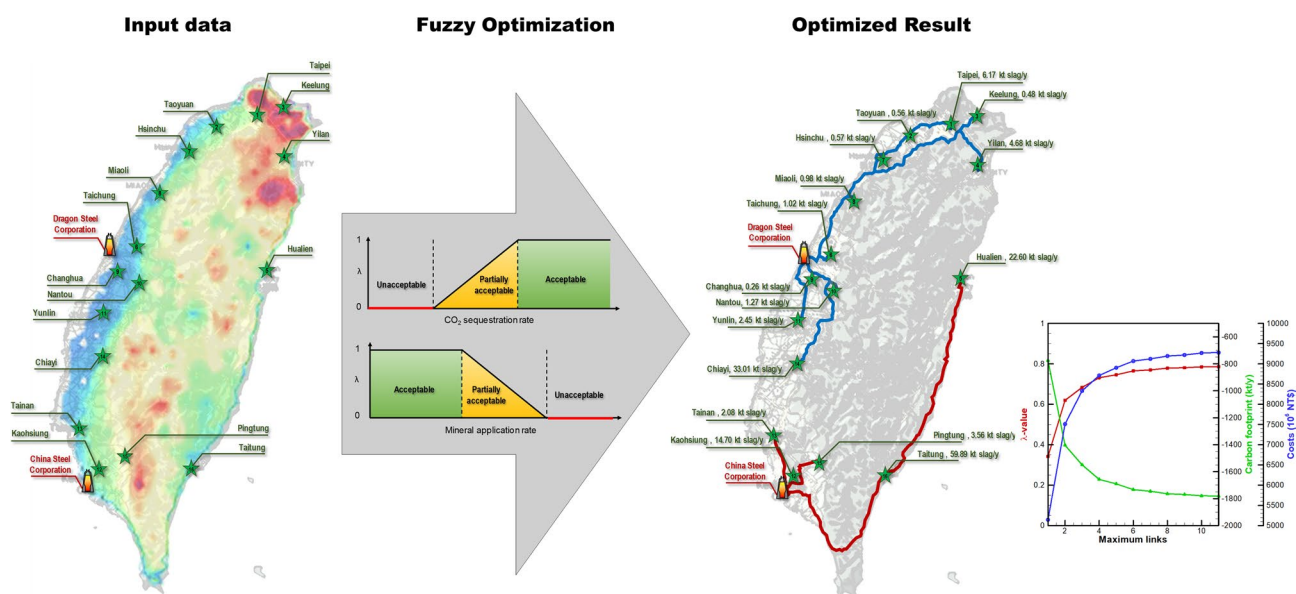
Received: 14 October 2020 / Accepted: 10 February 2021

© The Author(s), under exclusive licence to Springer-Verlag GmbH, DE part of Springer Nature 2021

Abstract

Enhanced weathering is a negative emissions technology based on the accelerated weathering of alkaline minerals. Such materials can be reduced to a fine powder and applied to land sinks to maximize the area exposed for reaction with rainwater and dissolved CO₂. The carbon is captured in the form of bicarbonate ions in the runoff, which ultimately carries it to the ocean for virtually permanent sequestration. Enhanced weathering has been demonstrated in proof-of-concept laboratory and field tests, but scale-up to a level that delivers significant CO₂ removal is still an engineering challenge that requires a system-level perspective. Future enhanced weathering networks should be planned like industrial supply chains, taking into account constraints in the supply of alkaline minerals and the availability of land sinks. Optimization of such networks should also take into account techno-economic uncertainties that are inherent in any emerging technology. To fill this research gap, this work develops a fuzzy mixed-integer linear programming model for optimal planning of enhanced weathering networks. The model is capable of handling multiple conflicting objectives and accounting for system uncertainties. The use of the model is illustrated with two case studies. First, a pedagogical example is solved; then, the model is demonstrated for a realistic scenario which shows that 0.69% of Taiwan's CO₂ emissions can be offset by the use of blast furnace slag for enhanced weathering.

Graphical abstract



Keywords Carbon dioxide removal (CDR) · Negative emissions technology (NET) · Enhanced weathering (EW) · Carbon management network (CMN) · Fuzzy mixed-integer linear programming (FMILP) · Circular economy (CE)

Extended author information available on the last page of the article

Introduction

The urgent challenge of managing global greenhouse gas (GHG) emissions needs to be met in order to prevent catastrophic temperature rise (IPCC 2018). Well-established measures to reduce carbon dioxide (CO₂) emissions, including energy efficiency enhancement and use of renewable energy, will need to be ramped up rapidly. Large-scale deployment of CO₂ capture and storage (CCS) and negative emissions technologies (NETs) will also be needed to reduce GHG emissions to zero by 2050 (Haszeldine et al. 2018). Rapid scale-up of these carbon management measures is needed to limit warming by the end of the century to below 2 °C (Winning et al. 2018). NETs remove CO₂ from the atmosphere via different physical, chemical and biological pathways and store the carbon permanently in a physical compartment. NETs include bioenergy with CCS (BECCS), direct air capture (DAC), biochar application, ocean liming, ocean fertilization, and enhanced weathering (EW). NETs are emerging technologies fraught with different levels of techno-economic uncertainties that are inherent in unproven systems. A comparative assessment of NET options based on carbon sequestration potential, cost, and technology readiness level (TRL) was done by McLaren (2012). In a series of review papers on NETs, Minx et al. (2018) surveyed the research landscape, Fuss et al. (2018) evaluated GHG abatement potential and risks, and Nemet et al. (2018) discussed their commercialization prospects. Other works have assessed the potential of NETs for carbon management. Alcalde et al. (2018) evaluated the potential of NETs in Scotland and reported the potential to achieve zero net GHG emissions. Similar studies have been done for the UK (Smith et al. 2016b), Ireland (McGeever et al. 2019), and the global scenarios (Smith et al. 2016a). In these works, the role of land, water, energy, and nutrient footprints as constraints on large-scale deployment of NETs was considered. The potential impacts of NETs on ecosystem services and the Sustainable Development Goals (SDGs) were assessed by Smith et al. (2019). Tan et al. (2020) proposed that Process Integration (PI) concepts can be applied to the problem of maximizing CO₂ removal (CDR) under such footprint constraints.

Compared to NETs such as DAC or BECCS, EW has the advantage that its technological components are already mature; only large-scale system integration remains unproven. Smith et al. (2016a) estimate the global potential of EW to reach 1 Gt CO₂/y by the end of the century, with land, energy, and water footprints of 10 Mha, 46 EJ/y, and 0.3 km³/y, respectively. Such footprints appear to be the limiting factor in the negative emissions potential of EW. Although there is an extensive body of literature on the fundamental science of EW as a NET, there has been minimal

work on engineering aspects that will be needed for significant future scale-up. In particular, mathematical models will be essential to support the planning of EW networks in the future (Lefebvre et al. 2019). Tan and Aviso (2019) proposed for EW systems to be treated as supply chains and developed a linear programming (LP) model to match mineral sources with land sinks. The LP formulation is based on PI models that have proven to be useful for planning various low-carbon systems (Klemeš et al. 2019).

One of the major branches of PI is Pinch Analysis (PA), which was originally developed to maximize the energy efficiency of process plants through heat recovery (Linnhoff, et al. 1982). Applications of PA have diversified significantly in the past four decades (Klemeš et al. 2018). Other than PA, Mathematical Programming (MP) (Klemeš and Kravanja 2013) and process graphs (P-graph) (Friedler et al. 2019) also play important roles as essential PI tools for the planning of sustainable industrial systems. Escalating concern about climate change has also led to the emergence of the PI subtopic of Carbon Management Networks (CMNs) (Tan and Foo 2018). EW networks as described by Tan and Aviso (2019) are a special class of CMNs; however, the current LP model lacks the capability to control network topology and cannot account for epistemic uncertainties that are present in EW systems. The absence of models to aid in the planning of future EW networks as a carbon management strategy is a clear research gap.

To address this research gap, a fuzzy mixed-integer linear programming (FMILP) model is developed in this work for optimizing EW networks. The formulation extends the LP model developed by Tan and Aviso (2019) to account for constraints imposed by network topology and epistemic uncertainties. The introduction of binary variables allows network topology to be controlled (Poplewski et al. 2010) and enables the identification of n-best near-optimal solutions (Voll et al. 2015). Fuzzy goals and constraints, on the other hand, are introduced to allow epistemic uncertainties in EW networks to be reflected in the model (Zimmermann 1978). The rest of the paper is organized as follows. The current literature on EW is reviewed in Sect. 2. The formal problem statement is given in Sect. 3. Then, the FMILP model formulation is given in Sect. 4. To illustrate the use of the model, a pedagogical example is solved in Sect. 5, followed by a case study in Sect. 6 on the use of blast furnace slag for EW in Taiwan. Finally, conclusions and prospects for further research are discussed in Sect. 7.

Literature review on enhanced weathering

Seifritz (1990) first proposed the possibility of sequestering CO₂ through accelerated reaction with silicate-bearing rocks. Laboratory-scale viability of EW was then demonstrated by

Kojima et al. (1997). EW can use either natural (e.g., basalt and olivine) or synthetic (e.g., metallurgical slag and cement waste) materials. Carbonic acid (dissolved CO_2) in rainwater reacts naturally with minerals such as silicates in a process known as weathering. The reactions sequester the carbon as dissolved bicarbonate ions or as solid carbonates. Any dissolved bicarbonate ions are eventually carried by run-off into bodies of water and ultimately to the ocean, where essentially permanent sequestration occurs. This very slow geological process can be accelerated to achieve significant CDR rates by reducing the minerals to a fine powder to increase the surface area for reaction. In ex situ terrestrial EW, this mineral powder can then be applied to land sinks at a rate that depends on factors including area, average precipitation, and ambient temperature (Moosdorf et al. 2014). Reaction stoichiometry determines the theoretical amount of CO_2 that is sequestered per unit mass of mineral. However, there are uncertainties involved in extrapolating theoretical estimates or laboratory test results to actual CDR rates in the field, due to the effects of factors such as particle size and soil conditions (Renforth et al. 2015). The mineral dissolution rate is a function of specific surface area and can be maximized by reducing particle size; however, the energy consumption and carbon footprint of grinding per unit mass of mineral also put a practical lower limit on particle size (Strefler et al. 2018). Alternative EW schemes include in situ terrestrial EW (e.g., Power et al. 2020) and coastal EW (Meysman and Montserrat 2017). The latter scheme relies on wave energy to provide agitation and accelerate the weathering of minerals such as olivine (Montserrat et al. 2017) or rocks such as basalt (Rigopoulos et al. 2018).

Positive or negative impacts of EW may occur at or in the vicinity of application sites. These impacts can manifest as

changes in the availability of ecosystem services to humans and have implications on achievement of the SDGs (Smith et al. 2019). Weathering reactions can alter soil chemistry in agricultural lands. Such changes may be beneficial, such as the increase in pH of acidic soil (Edwards et al. 2017). EW can also introduce additional nutrients such as phosphorus to soil, increasing the fertility of agricultural land and the biomass carbon stock of nonagricultural land (Hartmann et al. 2013). Such benefits can expand the role played by cropland in carbon management (Kantola et al. 2017). Alkaline run-off can also offset the acidification of marine ecosystems due to rising CO_2 concentration in the atmosphere (Bach et al. 2019). However, adverse impacts on soil fertility may also occur; mineral residue deposition can result when the application rate exceeds dissolution or runoff drainage rates (Pullin et al. 2019). Particulate matter (PM) emissions in the vicinity of application sites are also a potential environmental and health concern. Trace contaminants such as heavy metals in some industrial waste materials also pose risks. These issues may lead to limited social acceptability of EW as a carbon management strategy (Renforth 2012). In addition, the legal and regulatory aspects of EW systems still need to be examined (Webb 2020).

There have been multiple attempts to estimate the CDR potential of EW based on either mineral resource limits or land sink constraints. For example, Renforth (2012) estimated the cumulative EW potential in the UK at 430 Gt CO_2 based on mineral resource availability. Industrial solid waste also has significant potential as an EW resource and offers the further benefit of value-added utilization of residues under a Circular Economy (CE) framework. The annual global CDR potential of silicate-bearing industrial waste was originally estimated at 0.7–1.2 Gt/y CO_2 (Renforth et al. 2011). A more recent paper projects that this potential can reach 2.9–8.5 Gt/y CO_2 by 2100 (Renforth 2019). Due to

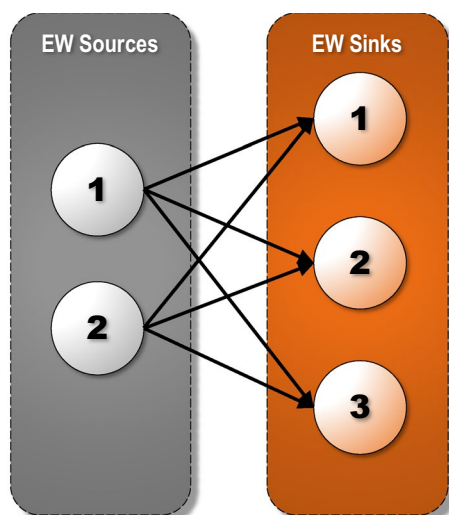


Fig. 1 Superstructure of an EW network

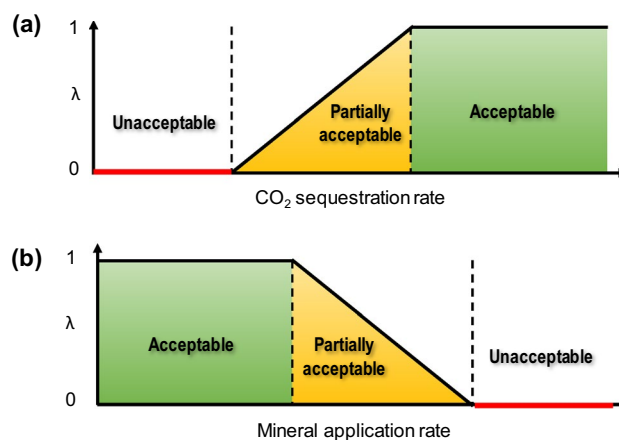


Fig. 2 Fuzzy membership functions for **a** CO_2 sequestration and **b** mineral application rates

the abundance of both natural and synthetic materials suitable for use in EW, the true potential may be limited by land and water footprints (Strefler et al. 2018). McLaren (2012) estimated the global potential of EW using olivine at about 1 Gt/y CO₂, at a cost of US\$ 20–40/t CO₂, considering land sink constraints. According to Beerling et al. (2020), the combined EW potential of Brazil, China, India, and USA is estimated at 0.5–2 Gt/y CO₂ based on cropland application. The corresponding costs were also estimated at US\$ 80–180/t CO₂. Lefebvre et al. (2019) estimated the potential of basalt EW in Sao Paulo State in Brazil at 1.3–2.4 Mt/y CO₂. McQueen et al. (2020) proposed a magnesium looping EW concept with an estimated CDR potential of 2–3 Gt/y CO₂ at a cost of US\$46–159/t CO₂. CDR estimates for EW systems show considerable variation, indicating the underlying techno-economic uncertainties. These uncertainties are epistemic in nature; they result from a fundamental lack of knowledge of the detailed chemical and physical mechanisms that affect the performance of EW in real systems (Beerling et al. 2020). Field tests are now being done to gain more information on the performance of EW when it is scaled up (e.g., Project Vesta 2020).

Estimates of the theoretical CDR potential of EW do not account for limitations that will occur in the implementation of engineered EW networks. PI principles can be used to develop techniques to optimize these systems (Tan et al. 2020). Except for the LP model proposed by Tan and Aviso (2019), there is a notable absence of decision support tools in the current literature to facilitate the planning of macro-scale EW systems. Such models will be needed in order to maximize the potential role of EW as a major carbon management strategy in the future (Tan and Aviso 2021). The development of an FMILP model in this work is intended to address this research gap.

Problem statement

The formal problem statement is as follows:

- Given m sources of EW minerals of known annual and cumulative capacity;
- Given n application sites with fuzzy annual and cumulative application rate limits;
- Given fuzzy CO₂ sequestration potentials of EW minerals;
- Given deterministic costs of acquiring, transporting, and applying EW minerals;
- Given other user-specified constraints on the topology of the CMN.

The problem is to determine the optimal allocation of EW minerals to application sites which maximizes CDR, taking

into account epistemic uncertainties in application rates and sequestration potential characteristics. The problem is similar to conventional supply chain network optimization (Tan and Aviso 2019), as shown in Fig. 1.

Optimization model

Zadeh (1965) first proposed fuzzy set theory as a branch of set theory that allows objects to have partial degrees of membership in sets. The degree of membership in any given fuzzy set is described by a membership function. Bellman and Zadeh (1970) then proposed the concept of fuzzy decision-making as the identification of the “confluence” (intersection) of fuzzy goals (or objectives) with fuzzy constraints. In this framework, the fuzzy solution represents the best compromise among potentially conflicting fuzzy goals and soft constraints, for which partial violation can be tolerated. This powerful concept led to subsequent growth in the use of fuzzy set theory for optimization in the presence of epistemic uncertainty. Based on this definition, a generic fuzzy MP formulation was then proposed by Zimmermann (1978) using max–min aggregation. In max–min aggregation, the optimal solution is the one that maximizes the satisfaction of the least satisfied fuzzy goal or constraint. The FMILP model developed in this work is based on the latter formulation. This class of fuzzy models has been applied to the design of sustainable systems such as water networks (Aviso et al. 2010), waste-to-energy networks (Taskhiri et al. 2015), effluent treatment processes (Choi and Park 2018), and CMNs (Aviso et al. 2020). A survey of applications to energy systems is given in a recent review paper (Arriola et al. 2020).

The formulation of Zimmermann (1978) is “symmetric,” with fuzzy goals and fuzzy constraints being mathematically indistinguishable. The optimal solution has the highest degree of membership in the fuzzy set defined by the aggregate of the fuzzy goals/constraints. The degree of membership in a fuzzy goal/constraint lies in the interval [0, 1]. A membership value of 0 represents nonsatisfaction (or violation), a value of 1 indicates full satisfaction, and fractional values indicate partial satisfaction. Linear membership functions as illustrated in Fig. 2 may be used for computational efficiency. In Fig. 2a, a piecewise linear membership function for the CO₂ sequestration rate is shown. In this case, higher values are considered more desirable (i.e., with membership values closer to 1). In Fig. 2b, a piecewise linear membership function is shown for the rock application rate, taking into account the risk of adverse effects on soil chemistry. In this case, lower values will incur lower risk and be seen as more desirable by a conservative decision-maker. Both types of membership functions can be present within the same model.

Nomenclature

Indices	
i	EW sources
j	EW sinks
Parameters	
α	Carbon sequestration factor
β	Carbon emission factor for transport
γ	Carbon emissions factor for crushing
δ	Carbon emissions factor for application
ϖ^A	Unit cost for crushing
ϖ^B	Unit cost for application
ϖ^C	Unit cost for transport
C_j	Maximum cumulative EW mineral application for sink j
CF^L	Fuzzy lower limit for system CO ₂ footprint
CF^U	Fuzzy upper limit for system CO ₂ footprint
$Cost^L$	Fuzzy lower limit for total cost
$Cost^U$	Fuzzy upper limit for total cost
D_j^L	Minimum EW mineral annual application rate at sink j
D_j^U	Maximum EW mineral annual application rate at sink j
M	Arbitrary large number
P_i	Operating life of source i
S_i	Annual capacity of available EW mineral from source i
x_{ij}	Distance between source i and sink j
Z	Maximum number of links from a source to sinks
Variables	
λ	Aggregate degree of membership
λ_j^A	Degree of satisfaction for application rate in sink j
λ^B	Degree of satisfaction for system cost
λ^C	Degree of satisfaction for system CO ₂ footprint
b_{ij}	Binary variable which indicates the activation ($b_{ij}=1$) or not ($b_{ij}=0$) of a link between source i and sink j
CF	Total CO ₂ footprint of the system
$Cost$	Total cost incurred by the system
D_j	Annual rate of application of mineral at sink j
r_{ij}	Annual rate of application of mineral from source i to sink j

The objective function is to maximize the aggregate degree of membership (λ) as shown in Eq. (1). The second term is the sum of the degrees of satisfaction of the individual fuzzy goals/constraints ($\lambda_j^A; \lambda^B; \lambda^C$) divided by an arbitrary large number and is included to ensure that the solution is Pareto optimal (Javadian et al. 2009). Using max–min aggregation, the degrees of satisfaction of the fuzzy goals/constraints are at least equal to the aggregate degree of membership, as indicated in Eqs. (2) to (4). The solution should meet the source capacity constraints as indicated in Eq. (5), where r_{ij} is the annual rate of EW mineral from source i applied to sink j , and S_i is the annual capacity of EW mineral from source i . Equation (6), on the other hand, sets a limit to the total annual rate of rock (or mineral) applied to sink $j - D_j$, which must be between the upper and lower fuzzy limits as indicated in Eq. (7). Furthermore, Eq. (7) reflects a risk-averse perspective that seeks to limit the application rate. Equation (8) ensures that the cumulative amount of EW mineral applied at each sink over the planning horizon of the source (P_i) does not exceed the cumulative capacity of sink j (C_j). Equation (9) accounts for the total CO₂ footprint of the system (CF), including the carbon sequestered by the

Table 1 Limiting data for sources (Tan and Aviso 2019)

Sources	Rock quantity (kt)	Rock flow rate (kt/y)	Operating life (y)
1	25	1.00	25
2	40	2.00	20
3	75	2.50	30

Table 2 Limiting data for sinks (adapted from Tan and Aviso 2019)

Sinks	Rock quantity (kt)	Fuzzy limits for rock flow rate (kt/y)		Operating life at maximum operation (y)
		Lower limit	Upper limit	
D1	4	0.02	0.40	10
D2	16	0.45	0.80	20
D3	20	0.70	1.00	20
D4	15	0.12	0.60	25
D5	160	1.00	4.00	40

Table 3 Distance between source and sink (in km)

Sources	D1	D2	D3	D4	D5
1	25	160	95	45	75
2	170	15	70	80	65
3	30	150	180	175	190

application of EW mineral, and the GHG emissions from crushing, transporting, and applying the EW minerals. Parameter α corresponds to the CO₂ sequestration potential of the EW minerals, β is the carbon emission factor of transport, γ is the emission factor of crushing, δ is the emission factor of application, and x_{ij} is the distance between source i and sink j . The fuzzy goal for CF is defined such that the degree of satisfaction λ^C approaches 1 as CF approaches the lower limit CF^L and approaches 0 as CF approaches the upper limit CF^U [as indicated in Eq. (10)]. Then, Eq. (11) accounts for the total system cost, where ϖ^A , ϖ^B , and ϖ^C are the cost factors associated with crushing, application, and transport, respectively. The fuzzy membership function for cost is given by Eq. (12), where $Cost^L$ and $Cost^U$ correspond to the lower and upper fuzzy limits for cost. Computations for CF and cost are structurally similar. Equation (13) indicates whether the link between source i and sink j is activated ($b_{ij}=1$) or not ($b_{ij}=0$) using a big-M constraint. The binary variables allow the inclusion of case-specific topological constraints such as flow rate limits [Eq. (14)], maximum number of branching, Z [Eq. (15)], incompatible or forbidden links [Eq. (16)], and necessary connections [Eq. (17)]. Equation (18) defines b_{ij} as a binary variable.

$$\max \lambda + \frac{1}{M} \left(\sum_j \lambda_j^A + \lambda^B + \lambda^C \right) \quad (1)$$

$$\lambda \leq \lambda_j^A \quad \forall j \quad (2)$$

$$\lambda \leq \lambda^B \quad (3)$$

$$\lambda \leq \lambda^C \quad (4)$$

$$\sum_{j=1}^n r_{ij} \leq S_i \quad \forall i \quad (5)$$

$$\sum_{i=1}^m r_{ij} \leq D_j \quad \forall j \quad (6)$$

$$D_j = D_j^U - \lambda_j^A (D_j^U - D_j^L) \quad \forall j \quad (7)$$

$$\sum_{i=1}^m P_i r_{ij} \leq C_j \quad \forall j \quad (8)$$

$$CF = \sum_{j=1}^n \sum_{i=1}^m (\alpha + \gamma + \delta + \beta x_{ij}) P_i r_{ij} \quad (9)$$

$$CF = CF^U - \lambda^C (CF^U - CF^L) \quad (10)$$

Table 4 Optimal allocation of crushed rock for Scenario 1 with $\lambda=0.7156$ (values in kt/y)

Sources	D1	D2	D3	D4	D5	Total
1			0.6637	0.2565	0.0798	1.0000
2		0.0487	0.0241			0.0728
3	0.1281	0.5009	0.0975		1.7735	2.5000
Total	0.1281	0.5496	0.7853	0.2565	1.8533	3.5728

Table 5 Optimal allocation of crushed rock in kt/y (r_{ij}) for Scenario 2 with $\lambda=0.7087$

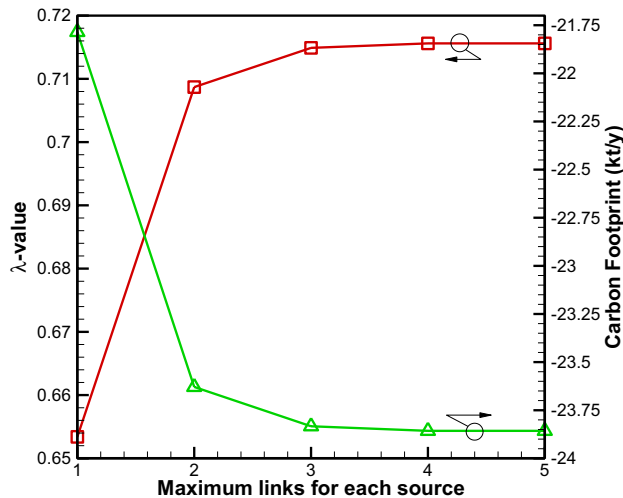
Sources	D1	D2	D3	D4	D5	Total
1			0.7402	0.2598		1.0000
2	0.1307		0.0472			0.1779
3		0.5333			1.8738	2.4071
Total	0.1307	0.5333	0.7874	0.2598	1.8738	3.5852

Table 6 Near-optimal allocation of crushed rock in kt/y (r_{ij}) for Scenario 2 with $\lambda=0.7046$

Sources	D1	D2	D3	D4	D5	Total
1			0.7382	0.2618		1.0000
2	0.1322					0.1322
3		0.5333			1.8860	2.4193
Total	0.1322	0.5333	0.7382	0.2618	1.8860	3.5515

Table 7 Summary of results for varying topological constraint in Case Study 1

Maximum links for each source (Z)	λ	CO ₂ footprint (kt/y)
Unlimited	0.7156	− 23.8571
4	0.7156	− 23.8571
3	0.7149	− 23.8333
2	0.7087	− 23.6289
1	0.6534	− 21.7849


Fig. 3 Resulting optimal solution for varying topological constraints for Case Study 1

$$\text{Cost} = \sum_{j=1}^n \sum_{i=1}^m (\varpi^A + \varpi^B + \varpi^C x_{ij}) P_i r_{ij} \quad (11)$$

$$\text{Cost} = \text{Cost}^U - \lambda^B (\text{Cost}^U - \text{Cost}^L) \quad (12)$$

Table 8 Limiting data for the sources

	Sources	Design capacity ^a (Mt crude steel/y)	Quantity of crude steel (Mt)	Slag flow rate (Mt/y)	Operating life (y)
Dragon Steel Corporation	1	2.50	75.0	1.00	30
	2	2.50	75.0	1.00	30
China Steel Corporation	3	1.93	57.9	0.77	30
	4	2.41	72.3	0.96	30
	5	2.65	79.5	1.06	30
	6	2.51	75.3	1.00	30

^aIndustrial Development Bureau (2020)

$$r_{ij} \leq b_{ij} M \quad \forall i, j \quad (13)$$

$$b_{ij} F_{ij}^L \leq r_{ij} \leq b_{ij} F_{ij}^U \quad \forall i, j \quad (14)$$

$$\sum_{j=1}^n b_{ij} \leq Z \quad \forall i \quad (15)$$

$$b_{ij} = 0 \quad (16)$$

$$b_{ij} = 1 \quad (17)$$

$$b_{ij} \in \{0, 1\} \quad \forall i, j \quad (18)$$

This FMILP model can be readily implemented in any optimization software with the capability to handle MILPs. Global optimality is guaranteed through the use of the branch-and-bound algorithm in such software. In this work, the software used is LINGO (Schrage and LINDO Systems, Inc., 1997); the examples that follow are solved in negligible time using a PC with Intel® Core™ i7-6500U 2.5 GHz CPU with 8.0 GB RAM.

Case Study 1: pedagogical example

This case study is adapted from the basalt application example of Tan and Aviso (2019). Costs are not considered in this pedagogical example. The data for the sources and sinks are given in Tables 1 and 2, respectively. The CO₂ sequestration potential is $\alpha = -0.3$ kt CO₂/kt rock. The distances between sources and sinks (x_{ij}) are shown in Table 3. In this case study, calculations were based on an emissions factor of $\beta = 0.1$ kg CO₂/t/km (Tan 2016). The emission factor associated with powder production is $\gamma = 0.0446$ kt CO₂/kt rock, while that for application is $\delta = 0.0054$ kt CO₂/kt rock (Strefler et al. 2018).

Table 9 Limiting data for sinks

Sinks	Place	Area (ha)	Rainfall ^a	Fuzzy limits for slag flow rate (kt/y)	
				Lower limit (D_j^L)	Upper limit (D_j^U)
1	Taipei	161.37	High	5.648	8.069
2	Taoyuan	17.32	Moderate	0.520	0.693
3	Keelung	12.58	High	0.440	0.629
4	Yilan	122.44	High	4.285	6.122
5	Hualien	703.31	Moderate	21.099	28.132
6	Taichung	37.57	Low	0.939	1.315
7	Hsinchu	21.16	Low	0.529	0.741
8	Miaoli	30.61	Moderate	0.918	1.224
9	Changhua	9.48	Low	0.237	0.332
10	Nantou	39.57	Moderate	1.187	1.583
11	Yunlin	76.13	Moderate	2.284	3.045
12	Kaohsiung	541.46	Low	13.537	18.951
13	Tainan	76.72	Low	1.918	2.685
14	Chiayi	1027.18	Moderate	30.815	41.087
15	Pingtung	110.87	Moderate	3.326	4.435
16	Taitung	2204.48	Low	55.112	77.157

^aApplication rates according to rainfall: low = 25–35 t/ha; moderate = 30–40 t/ha; high = 35–50 t/ha

The lower limit for the CO₂ footprint of the entire network was obtained by minimizing the CF using the largest possible application rate; this results in $CF^L = -33.34$ kt CO₂. On the other hand, the upper limit is taken as $CF^U = 0$ kt CO₂, corresponding to the case of not using EW at all. The fuzzy limits for the application rate are as indicated in Table 2.

Two different scenarios are considered here. In Scenario 1, there is no topological constraint on the network, while Scenario 2 considers topological constraints particularly on limiting the number of branching from sources to sinks as indicated in Eq. (15). For Scenario 1, Eq. (1) is solved subject to constraints in Eqs. (2) and (4) to (10). The resulting aggregate degree of membership is $\lambda = 0.7156$, which corresponds to $CF = -23.86$ kt CO₂. The optimal network together with the total application rates in the different sinks is shown in Table 4. The total available powdered rocks from S1 and S3 are completely used up, while that from S2 is only partially utilized. The sink with the highest potential for carbon sequestration is prioritized, with D5 receiving the largest amount of rock. The link between S3 and D5, for example, has the largest amount of rock application, despite having the highest associated transport emissions. This result indicates that the sequestration capability of powdered rock application offsets the CO₂ penalty from crushing, transport, and application. Note that, without any topological constraints, S3 is linked to four out of the five sinks. It is also important to note that the optimal satisficing solution simultaneously considers increasing the CO₂ sequestration and decreasing the application rates.

Additional scenarios were considered by reducing the maximum number of sinks each source can be linked to by defining a value for Z and solving Eq. (1) subject to Eqs. (2), (4) to (10), (13), (15), and (18). Imposing such a constraint results in a simpler network structure, which can result in economies of scale and reduced operational problems. Looking more closely at the scenario where the maximum number of links is 2 ($Z = 2$), the resulting network is shown in Table 5. This network has a slightly higher CO₂ footprint of $CF = -23.63$ kt CO₂ with an aggregate degree of membership of $\lambda = 0.7087$. It is also possible to identify near-optimal network structures, which can be obtained using mixed-integer cuts or cutting plane methods during optimization. An example of a near-optimal network is shown in Table 6, which results in a $CF = -23.49$ and a $\lambda = 0.7046$. Such alternative solutions provide options for the decision-maker and can be considered when deciding on the final CMN (Voll et al. 2015). For this particular case, the results show that the sequestered carbon of the near-optimal solution is just 0.6% lower than that achieved in the optimal solution. Furthermore, the network of the near-optimal solution has eliminated the link with the smallest amount of applied rock, thereby simplifying the network structure. A summary of the trade-off between the overall degree of satisfaction and CO₂ footprint as the number of links is reduced is given in Table 7. Such features should be taken in consideration when choosing the final structure.

Fig. 4 Geographic location of blast furnaces and sink sites together with rainfall intensity

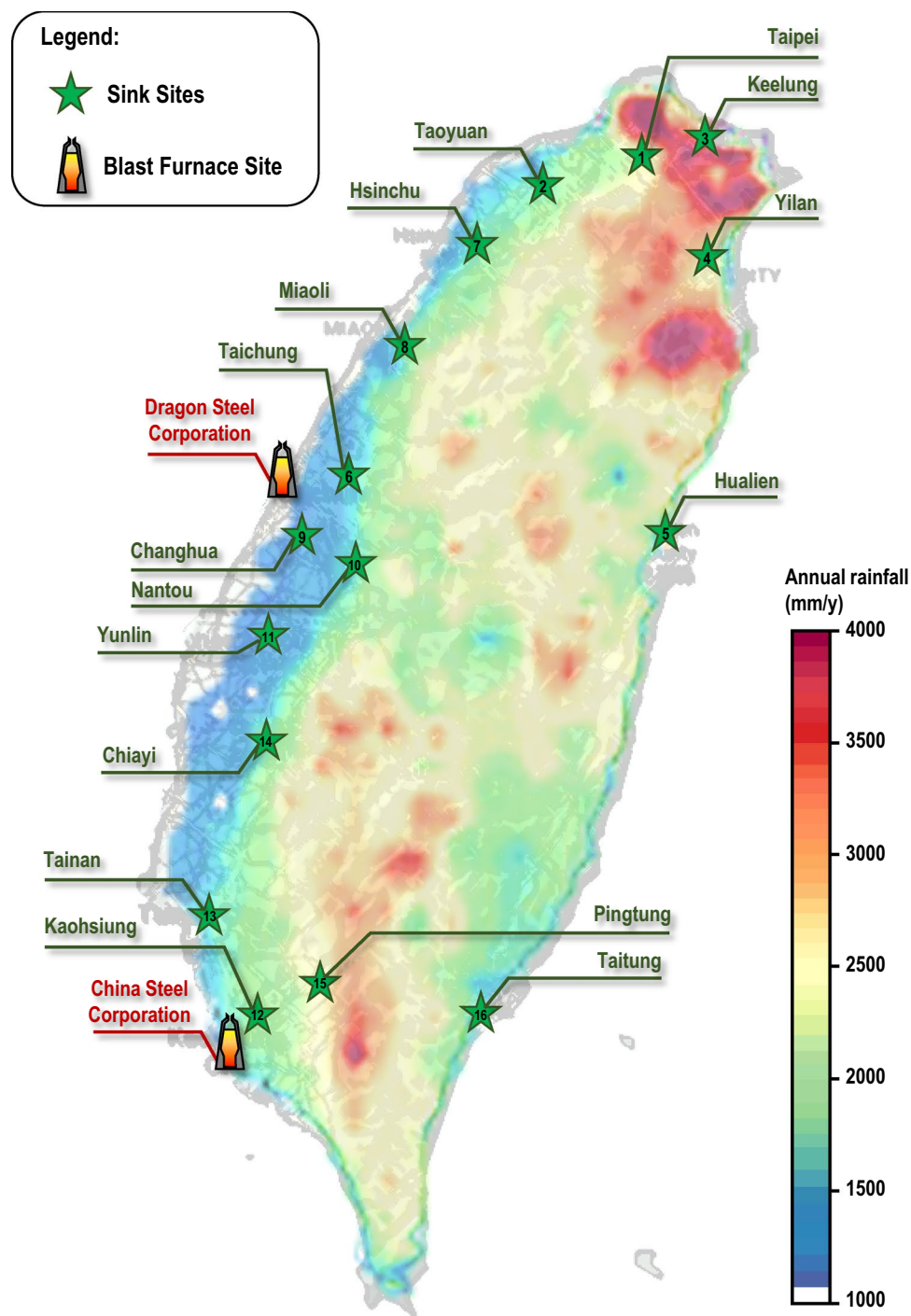


Figure 3 illustrates the trade-off between the overall degree of satisfaction and the CO₂ footprint obtained as a function of the topological constraints.

Case Study 2: EW with blast furnace slag in Taiwan

This case study considers the potential of using solid waste material for EW in Taiwan, a highly industrialized, land-constrained country. Use of industrial waste for EW can take advantage of large amounts of material which currently

Table 10 Problem coefficients

Emission factors	Value	Unit	Reference
A	-0.495	kt CO ₂ /kt	Renforth et al. (2011)
B	0.00006	kt CO ₂ /kt/km	Renforth (2012)
F	0.09	kt CO ₂ /kt	Renforth (2012)
Δ	0.011	kt CO ₂ /kt	Renforth (2012)
Cost coefficients	Value	Unit	References
ϖ^A	925	10 ³ NT\$/kt	Renforth (2012)
ϖ^B	780	10 ³ NT\$/kt	Streffer et al. (2018)
ϖ^C	2	10 ³ NT\$/kt/km	Renforth (2012)

Table 11 Distance from source to sink in km (x_{ij})

Sinks (j)	Source (i)	
	Dragon Steel Corporation	China Steel Corporation
1	163	359
2	156	336
3	198	386
4	223	414
5	327	326
6	28.9	218
7	103	289
8	73	259
9	27	222
10	61	191
11	86	157
12	215	13
13	174	80
14	110	126
15	233	24
16	379	151

Table 12 Fuzzy limits

Parameter	Lower limit	Upper limit
CO ₂ footprint (kt CO ₂)	-2266.17	0
Cost (10 ³ NT\$)	0	118,000,000

presents disposal problems (Renforth 2019). It can also help to address carbon management and CE goals concurrently (Klemeš et al. 2019). According to the World Steel Association (2020), Taiwan ranks twelfth in the world in crude steel production, accounting for 1.2% of the global production in 2019. The production of crude steel in Taiwan in 2019 was 22 Mt, of which 61.9% was produced by blast furnace processes. There are six blast furnaces in Taiwan, operated by two corporations. China Steel in Kaohsiung has four blast furnaces, and Dragon Steel in Taichung has two.

The total production capacity of these blast furnaces is 14.5 Mt/y. Blast furnace slag is the main by-product of the blast furnace processes and is mostly granulated to produce slag powder, with a small portion being used to make engineering materials. Alternatively, powdered blast furnace slag may be used for EW, in which case marginal land in Taiwan can be the sinks.

Table 8 provides data on the capacity of each blast furnace together with the expected amount of slag generated from the process, under the assumption that 0.25 t of slag is generated per ton of crude steel processed, which is at the lower end of the typical value. Literature suggests that 0.25–1.20 t of slag is generated per ton of crude steel (Renforth 2011). Table 9, on the other hand, identifies available marginal land in Taiwan and includes data on the land area available as well as an indication of the typical rainfall experienced in the region. The amount of precipitation can greatly influence the slag application limit for the marginal land. In this case, the marginal lands have been classified according to the rainfall. This classification was then utilized to identify the lower and upper fuzzy limits for mineral rock or slag application. According to Alcalde et al. (2018), application rates are typically within 10 to 50 t/ha/y, with the lower limit corresponding to the maximum application rate for agricultural land. Thus, for marginal land receiving low levels of precipitation, a range of 25 to 35 t/ha/y is used; for moderate precipitation, application rates are assumed to range between 30 and 40 t/ha/y, while a range of 35 to 50 t/ha/y is used for marginal lands with high levels of precipitation. The lower and upper fuzzy limits for the slag flow rate were then determined based on the lower and upper application rates and the total area covered by the marginal land. Figure 4 shows the geographic location of blast furnaces and the sink sites are represented by the starred locations, while the color intensity of the regions represents rainfall intensity as taken from Kuo et al. (2016).

Other coefficients are summarized in Table 10 (note that US\$ 1 = NT\$ 30), while the distances between the blast furnaces and the marginal lands are given in Table 11.

The fuzzy limits for the CO₂ footprint and cost were obtained by determining independently the lowest possible cost and the lowest possible CO₂ footprint that the system can achieve, respectively. The lowest possible CO₂ footprint was obtained by optimizing the network with the objective of minimizing the total CO₂ footprint of the system, while the upper limit corresponds to the baseline scenario which does not implement EW. The upper limit for the cost, on the other hand, is the associated cost for minimizing the CO₂ footprint of the system, including the crushing, transport, and application of slag. The lower limit for cost refers to the baseline case which does not make use of EW and thus does not incur any additional costs from the baseline. These limits are summarized in Table 12.

Table 13 Optimal network in kt slag/y with $\lambda = 0.7861$

Sinks	Source					
	Dragon Steel Corporation		China Steel Corporation			
	1	2	3	4	5	6
1	6.17					
2	0.56					
3	0.48					
4	4.68					
5				22.60		
6	1.02					
7	0.57					
8	0.98					
9	0.26					
10	1.27					
11	2.45					
12				14.70		
13				2.08		
14	33.01					
15				3.56		
16				59.83		

Solving Eq. (1) subject to constraints in Eqs. (2) to (13) and (18) results in the optimal network shown in Table 13. In this network, the system achieves a CO₂ footprint of −1781.22 kt CO₂ and incurs a cost of NT\$ 9278 million with the optimal geographic route shown in Fig. 5, where the starred locations correspond to the application sites. Figure 5 is a visual representation of the optimal network shown in Table 13. Dragon Steel Corporation (DSC) applies powdered slag to 11 different sites, while China Steel Corporation (CSC) applies to only five. Nonetheless, the total amount of slag applied from DSC only accounts for 33% of the total slag applied by the system, while CSC makes up the remaining 67%. One of the reasons for this is that DSC is located closer to sinks which have smaller capacities, while CSC is closer to sinks with higher capacities. However, the structure also indicates that none of the sinks has been fully utilized.

If topological constraints are again imposed such that each of the companies (i.e., DSC and CSC) can only apply slag to a maximum of four different application sites, the optimal solution [obtained by solving Eq. (1) subject to constraints in Eqs. (2) to (13), (15) and (18)] is as shown in Table 14. In this network, the system achieves a higher CO₂ footprint of −1657.27 kt CO₂ and incurs a lower cost of 8711 million NT\$ with optimal geographic route shown in Fig. 6. Furthermore, the number of application sites selected has been reduced with DSC applying to four different sites and CSC applying to just two.

Table 15 provides a summary of the trade-off between the achieved overall degree of satisfaction, CO₂ footprint and cost when topological constraints are imposed on the source–sink matching. Figure 7 shows the trend of the trade-off between these three factors. The number of links listed in the first column corresponds to the maximum number of application sites that each steel company can deliver its slag to. Increasing the number of allowable links reduces the CO₂ footprint but increases costs. The lowest increase in cost per t of additional CO₂ sequestered occurs when the number of allowable links is increased from 3 to 4. The highest additional cost per t of additional CO₂ sequestered occurs when the number of allowable links is increased from 4 to 5. Such analysis provides insights on the practical implementation of EW networks and allows decision-makers to clearly examine the relation between CO₂ sequestration, cost, and network complexity. The optimal sequestration cost is NT\$ 5209/t CO₂ (or US\$ 174/t CO₂), which indicates the level of carbon tax needed to make the system economically viable.

The case study results show that an optimal EW network using only blast furnace slag has the potential to reduce Taiwan's CO₂ emissions, currently at 259 Mt/y (Bureau of Energy 2020), by 0.69%. Although this may seem like a very small reduction, this example accounts for just one type of industrial waste. Similar principles can be applied to the use of other industrial solid waste for EW. Examples include slag from downstream steel production, cement kiln dust, coal ash from power plants, red mud from primary aluminum smelting, and construction or demolition waste

Fig. 5 Resulting optimal network route for $\lambda = 0.7861$



(Renforth 2019). Use of such residues in EW can result in a synergy between CE and carbon management goals via PI methodology (Klemeš et al. 2019). The main limitation is that the application of industrial waste may be restricted only to marginal lands, since the risk of introducing trace contaminants (e.g., heavy metals) to agricultural land may be

socially or environmentally unacceptable. Use of naturally occurring EW minerals found in rocks such as basalt may be more acceptable. This option will allow much higher levels of CDR in land-constrained countries such as Taiwan, due to the abundance of potential EW minerals in igneous rocks (Lu et al. 2011).

Table 14 Optimal network in kt slag/y with $\lambda=0.7313$ (with topologic constraint, each company can only apply in a maximum of four different application sites)

Sinks	Source					
	Dragon Steel Corporation			China Steel Corporation		
	1	2	3	4	5	6
1		6.30				
2						
3						
4		4.78				
5		22.99				
6						
7						
8						
9						
10						
11						
12				14.99		
13						
14		33.58				
15						
16						61.04

Conclusions

In this work, a novel FMILP model was developed for optimal planning of EW networks. The model takes into account uncertainty in terrestrial sink application rate limits using fuzzy set theory. Binary variables in the model allow identification of n-best near-optimal solutions and customization of the EW network topology. The model was first illustrated using a pedagogical example. A case study on EW using blast furnace slag in Taiwan was then solved to demonstrate its capability with a realistic scenario. The case study also illustrates the potential to integrate CDR and CE goals within a single optimized system. The model itself is generic and can be used with a broad range of natural or synthetic materials suitable for EW. Most previous studies on EW have focused on its potential to sequester carbon but

have not addressed its optimal implementation or large-scale deployment. This model represents a significant contribution to the EW literature by providing the capability to plan large-scale EW networks while balancing negative emission goals with mineral application limits. Such a capability will be needed in order to maximize the potential of EW as a globally significant NET in the future.

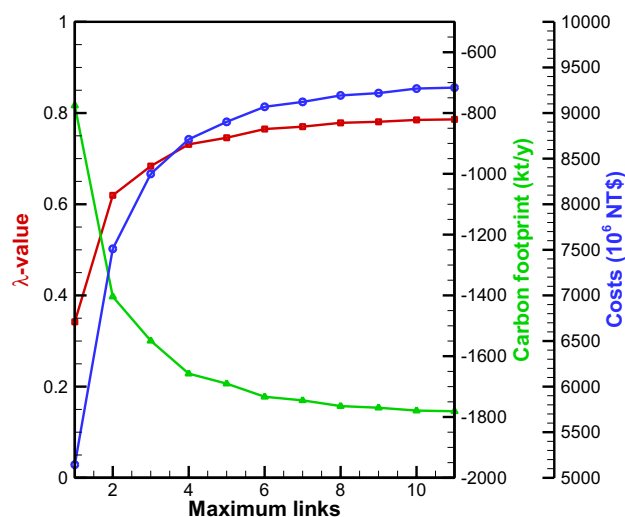
Future work can extend this work to account for EW network revamp as required by changing conditions. Alternative or hybrid optimization approaches based on P-graph or Pinch Analysis can also be developed. Emphasis should be placed on reducing unit CDR cost to make such systems economically viable. The model can also be applied to other geographic contexts considering locally available EW minerals.

Fig. 6 Resulting optimal network route for $\lambda = 0.7313$



Table 15 Summary of results for varying topological constraint in Case Study 2

Maximum links for each company	λ	CO ₂ footprint (kt/y)	Cost (10 ⁶ NT\$/y)
Unlimited	0.7861	−1781.22	9278.34
10	0.7849	−1778.84	9268.13
9	0.7808	−1769.41	9218.72
8	0.7785	−1764.14	9193.11
7	0.7701	−1745.24	9122.20
6	0.7649	−1733.39	9068.43
5	0.7458	−1690.19	8903.39
4	0.7313	−1657.27	8711.48
3	0.6836	−1549.21	8332.89
2	0.6195	−1403.90	7511.21
1	0.3421	−775.35	5143.81

**Fig. 7** Resulting optimal solution for varying the topological constraints for Case Study 2

Declarations

Conflict of interest The authors declare that we have no known competing financial interests or personal relationships that could have influenced the work reported in this paper.

References


- Alcalde J, Smith P, Haszeldine RS, Bond CE (2018) The potential for implementation of Negative Emission Technologies in Scotland. *Int J Greenhouse Gas Control* 76:85–91
- Arriola ER, Ubando AT, Chen W-H (2020) A bibliometric review on the application of fuzzy optimization to sustainable energy technologies. *Int J Energy Res*. <https://doi.org/10.1002/er.5729>
- Aviso KB, Sy CL, Tan RR, Ubando AT (2020) Fuzzy optimization of carbon management networks based on direct and indirect biomass co-firing. *Renew Sustain Energy Rev* 132. Article 110035
- Aviso KB, Tan RR, Culaba AB, Cruz JB Jr (2010) Bi-level fuzzy optimization approach for water exchange in eco-industrial parks. *Process Saf Environ Prot* 88:31–40
- Bach LT, Gill SJ, Rickaby REM, Gore S, Renforth P (2019) CO₂ removal with enhanced weathering and ocean alkalinity enhancement: potential risks and co-benefits for marine pelagic ecosystems. *Front Clim* 1. Article 7
- Beerling DJ, Kantzas EP, Lomas MR, Wade P, Eufrazio RM, Renforth P, Sarkar B, Andrews MG, James RH, Pearce CR, Mercure J-F, Pollitt H, Holden PB, Edwards NR, Khanna M, Koh L, Quegan S, Pidgeon NF, Janssens IA, Hansen J, Banwart SA (2020) Potential for large-scale CO₂ removal via enhanced rock weathering with croplands. *Nature* 583:242–248
- Bellman RE, Zadeh LA (1970) Decision-making in a fuzzy environment. *Manage Sci* 17:B141–B147
- Bureau of Energy, Ministry of Economic Affairs (2020) Greenhouse gases. https://www.moeaboe.gov.tw/ECW/populace/content/SubMenu.aspx?menu_id=114. Accessed 27 Aug 2020
- Choi AES, Park H-S (2018) Fuzzy multi-objective optimization case study based on an anaerobic co-digestion process of food waste leachate and piggery wastewater. *J Environ Manage* 223:314–323
- Edwards DP, Lim F, James RH, Pearce CR, Scholes J, Freckleton RP, Beerling DJ (2017) Climate change mitigation: Potential benefits and pitfalls of enhanced rock weathering in tropical agriculture. *Biol Lett* 13:0715
- Friedler F, Aviso KB, Bertok B, Foo DCY, Tan RR (2019) Prospects and challenges for chemical process synthesis with P-graph. *Curr Chem Eng* 26:58–64
- Fuss S, Lamb WF, Callaghan MW, Hilaire J, Creutzig F, Amann T, Beringer T, De Oliveira Garcia W, Hartmann J, Khanna T, Luderer G, Nemet GF, Rogelj J, Smith P, Vicente Vicente JL, Wilcox J, Del Mar Zamora Dominguez M, Minx JC (2018) Negative emissions—part 2: costs, potentials and side effects. *Environ Res Lett* 13. Article 063002
- Hartmann J, West AJ, Renforth P, Köhler P, De La Rocha CL, Wolf-Gladrow DA, Dürr HH, Scheffran J (2013) Enhanced chemical weathering as a geoengineering strategy to reduce atmospheric carbon dioxide, supply nutrients, and mitigate ocean acidification. *Rev Geophys* 51:113–149
- Haszeldine RS, Flude S, Johnson G, Scott V (2018) Negative emissions technologies and carbon capture and storage to achieve the Paris agreement commitments. *Philos Trans R Soc A Math Phys Eng Sci* 376. Article 20160447
- Industrial Development Bureau, Ministry of Economic Affairs (2020) 2020 Industrial Development in Taiwan. C. The Bureau, Taipei, Taiwan, R.O.C, R.O
- Intergovernmental Panel on Climate Change (2018) Summary for policymakers. In Masson-Delmotte V, Zhai P, Pörtner HO, Roberts D, Skea J, Shukla PR, Pirani A, Moufouma-Okia W, Péan C, Pidcock R, Connors S, Matthews JBR, Chen Y, Zhou X, Gomis MI, Lonnoy E, Maycock T, Tignor M, Waterfield T (eds) *Global warming of 1.5 °C. An IPCC special report on the impacts of global warming of 1.5 °C above pre-industrial levels and related global greenhouse gas emission pathways, in the context of strengthening the global response to the threat of climate change, sustainable development, and efforts to eradicate poverty*. World Meteorological Organization, Geneva, Switzerland
- Kantola IB, Masters MD, Beerling DJ, Long SP, DeLucia EH (2017) Potential of global croplands and bioenergy crops for climate change mitigation through deployment for enhanced weathering. *Biol Lett* 13. Article 20160714

- Javadian N, Maali Y, Mahdavi AN (2009) Fuzzy linear programming with grades of satisfaction in constraints. *Iran J Fuzzy Syst* 6:17–35
- Klemeš JJ, Kravanja Z (2013) Forty years of heat integration: pinch analysis (PA) and mathematical programming (MP). *Curr Opin Chem Eng* 2:461–474
- Klemeš JJ, Varbanov PS, Walmsley TG, Foley A (2019) Process integration and circular economy for renewable and sustainable energy systems. *Renew Sustain Energy Rev* 116. Article 109435
- Klemeš JJ, Varbanov PS, Walmsley TG, Jia X (2018) New directions in the implementation of Pinch Methodology (PM). *Renew Sustain Energy Rev* 98:439–468
- Kojima T, Nagamine A, Ueno N, Uemiya S (1997) Absorption and fixation of carbon dioxide by rock weathering. *Energy Convers Manage* 38:S461–S466
- Kuo Y-C, Lee M-A, Lu M-M (2016) Association of Taiwan's October rainfall patterns with large-scale oceanic and atmospheric phenomena. *Atmos Res* 180:200–210
- Lefebvre D, Goglio P, Williams A, Manning DAC, de Azevedo AC, Bergmann M, Meersmans J, Smith P (2019) Assessing the potential of soil carbonation and enhanced weathering through life cycle assessment: a case study for Sao Paulo State, Brazil. *J Clean Prod* 233:468–461
- McLaren D (2012) A comparative global assessment of potential negative emissions technologies. *Process Saf Environ Prot* 90:489–500
- Linnhoff B, Townsend DW, Boland D, Hewitt GF, Thomas BEA, Guy AR, Marshall RH (1982) A user guide on process integration for the efficient use of energy. Institution of Chemical Engineers, Rugby
- Lu H-Y, Lin C-K, Lin W, Liou T-S, Chen W-F, Chang P-Y (2011) A natural analogue for CO₂ mineral sequestration in Miocene basalt in the Kuanhsi-Chutung area, Northwestern Taiwan. *Int J Greenh Gas Control* 5:1329–1338
- McGeever AH, Price P, McMullin B, Jones MB (2019) Assessing the terrestrial capacity for Negative Emission Technologies in Ireland. *Carbon Manag* 10:1–10
- McQueen N, Kelemen P, Dipple G, Renforth P, Wilcox J (2020) Ambient weathering of magnesium oxide for CO₂ removal from air. *Nat Commun* 11. Article 3299
- Meysman FJR, Montserrat F (2017) Negative CO₂ emissions via enhanced silicate weathering in coastal environments. *Biol Lett* 13. Article 20160905
- Minx JC, Lamb WF, Callaghan MW, Fuss S, Hilaire J, Creutzig F, Amann T, Beringer T, De Oliveira Garcia W, Hartmann J, Khanna T, Lenzi D, Luderer G, Nemet GF, Rogelj J, Smith P, Vicente JL, Wilcox J, Del Mar Zamora Dominguez M (2018) Negative emissions—part 1: research landscape and synthesis. *Environ Res Lett* 13. Article 063001
- Montserrat F, Renforth P, Hartmann J, Leermakers M, Knops P, Meysman FJR (2017) Olivine dissolution in seawater: Implications for CO₂ sequestration through enhanced weathering in coastal environments. *Environ Sci Technol* 5:3960–3972
- Moosdorf N, Renforth P, Hartmann J (2014) Carbon dioxide efficiency of terrestrial enhanced weathering. *Environ Sci Technol* 48:4809–4816
- Nemet GF, Callaghan MW, Creutzig F, Fuss S, Hartmann J, Hilaire J, Lamb WF, Minx JC, Rogers S, Smith P (2018) Negative emissions—part 3: innovation and upscaling. *Environ Res Lett* 13: Article 063003
- Poplewski G, Wałczyk K, Jeżowski J (2010) Optimization-based method for calculating water networks with user specified characteristics. *Chem Eng Res Des* 88:109–120
- Power IM, Dipple GM, Bradshaw PMD, Harrison AL (2020) Prospects for CO₂ mineralization and enhanced weathering of ultramafic mine tailings from the Baptiste nickel deposit in British Columbia, Canada. *Int J Greenh Gas Control* 94. Article 102895
- Project Vesta (2020) Turning the tide on climate change with green sand beaches. <https://projectvesta.org/>. Accessed on 10 Sept 2020
- Pullin H, Bray AW, Muir DD, Safford DJ, Mayes WM, Renforth P (2019) Atmospheric carbon capture performance of legacy iron and steel waste. *Environ Sci Technol* 53:9502–9511
- Renforth P, Washbourne C-L, Taylder J, Manning DAC (2011) Silicate production and availability for mineral carbonation. *Environ Sci Technol* 45:2035–2041
- Renforth P (2012) The potential of enhanced weathering in the UK. *Int J Greenhouse Gas Control* 10:229–243
- Renforth P, Pogge von Strandmann PAE, Henderson GM (2015) The dissolution of olivine added to soil: Implications for enhanced weathering. *Appl Geochem* 69:109–118
- Renforth P (2019) The negative emission potential of alkaline materials. *Nat Commun* 10. Article 1401
- Rigopoulos I, Harrison AL, Delimitis A, Ioannou I, Efstathiou AM, Kyratsi T, Oelkers EH (2018) Carbon sequestration via enhanced weathering of peridotites and basalts in seawater. *Appl Geochem* 91:197–207
- Schrage LE, Systems Inc LINDO (1997) Optimization modeling with LINGO. Duxbury Press, Bolinas
- Seifritz W (1990) CO₂ disposal by means of silicates. *Nature* 345:486
- Smith P, Davis SJ, Creutzig F, Fuss S, Minx J, Gabrielle B, Kato E, Jackson RB, Cowie A, Kriegler E, van Vuuren DP, Rogelj J, Ciais P, Milne J, Canadell JG, McCollum D, Peters G, Andrew R, Krey V, Shrestha G, Friedlingstein P, Gasser T, Grüber A, Heidug WK, Jonas M, Jones CD, Kraxner F, Littleton E, Lowe J, Moreira JR, Nakicenovic N, Obersteiner M, Patwardhan A, Rogner M, Rubin E, Sharifi A, Torvanger A, Yamagata Y, Edmonds J, Yongsung C (2016a) Biophysical and economic limits to negative CO₂ emissions. *Nature Climate Change* 6:42–50
- Smith P, Haszeldine RS, Smith SM (2016b) Preliminary assessment of the potential for, and limitations to, terrestrial negative emission technologies in the UK. *Environ Sci Process Impacts* 18:1400–1405
- Smith P, Adams J, Beerling DJ, Beringer T, Calvin KV, Fuss S, Griscom B, Hagemann N, Kammann C, Kraxner F, Minx JC, Popp A, Renforth P, Vicente JL, Keesstra S (2019) Land-management options for greenhouse gas removal and their impacts on ecosystem services and the sustainable development goals. *Annu Rev Environ Resour* 44:255–286
- Strefler J, Amann T, Bauer N, Kriegler E, Hartmann J (2018) Potential and costs of carbon dioxide removal by enhanced weathering of rocks. *Environ Res Lett* 13. Article 034010
- Tan RR (2016) A multi-period source-sink mixed integer linear programming model for biochar-based carbon sequestration systems. *Sustain Prod Consum* 8:57–63
- Tan RR, Aviso KB (2019) A linear program for optimizing enhanced weathering networks. *Results Eng* 3. Article 100028
- Tan RR, Aviso KB (2021) On life-cycle sustainability optimization of enhanced weathering systems. *J Clean Prod* 289. Article 125836
- Tan RR, Bandyopadhyay S, Foo DCY (2020) The role of process integration in managing resource constraints on negative emissions technologies. *Resour Conserv Recycl* 153. Article 104540
- Tan RR, Foo DCY (2018) Process integration and climate change: From carbon emissions pinch analysis to carbon management networks. *Chem Eng Trans* 70:1–6
- Taskhiri MS, Behera SK, Tan RR, Park H-S (2015) Fuzzy optimization of a waste-to-energy network system in an eco-industrial park. *J Mater Cycles Waste Manage* 17:476–489
- Voll P, Jennings M, Hennen M, Shah N, Bardow A (2015) The optimum is not enough: a near-optimal solution paradigm for energy systems synthesis. *Energy* 82:446–456
- Webb RM (2020) The law of enhanced weathering for carbon dioxide removal. Discussion paper, Sabin Center for Climate Change Law, Columbia Law School, USA

- Winning M, Pye S, Glynn J, Scamman D, Welsby D (2018) How low can we go? The implications of delayed ratcheting and negative emissions technologies on achieving well below 2 °C. In: Giannakidis G, Karlsson K, Labriet M, Ó Gallachóir B (eds) Limiting global warming to well below 2 °C: energy system modelling and policy development. Springer, Cham, pp 51–65
- World Steel Association (2020) World crude steel production. www.worldsteel.org. Retrieved 2020–08–08
- Zadeh LA (1965) Fuzzy Sets. *Inf Control* 8:338–353
- Zimmermann H-J (1978) Fuzzy programming and linear programming with several objective functions. *Fuzzy Sets Syst* 1:45–55

Publisher's Note Springer Nature remains neutral with regard to jurisdictional claims in published maps and institutional affiliations.

Authors and Affiliations

Kathleen B. Aviso¹  · Jui-Yuan Lee² · Aristotle T. Ubando³ · Raymond R. Tan¹

✉ Kathleen B. Aviso
kathleen.aviso@dlsu.edu.ph

¹ Chemical Engineering Department, De La Salle University,
2401 Taft Avenue, 0922 Manila, Philippines

² Department of Chemical Engineering and Biotechnology,
National Taipei University of Technology, Taipei 10608,
Taiwan

³ Mechanical Engineering Department, De La Salle University,
2401 Taft Avenue, 0922 Manila, Philippines